Structure and properties of titanium–zinc borophosphate glasses

Ladislav Koudelka[a,*], Petr Mošner[a], Jaroslav Pospíšil[a],
Lionel Montagne[b], Gerard Palavit[b]

[a]*Faculty of Chemical Technology, University of Pardubice, 532 10 Pardubice, Czech Republic*
[b]*Laboratoire de Cristallochimie et Physicochimie du Solide, Ecole Nationale Superieure de Chimie de Lille, BP108,
59652 Villeneuve d'Ascq Cedex, France*

Abstract

The structure of $50ZnO–10B_2O_3–40P_2O_5 + xTiO_2$ glasses prepared by slow cooling (for $x = 0$–24 mol% TiO_2) or by quenching (for $x = 28$–64 mol% TiO_2) was studied by Raman, ^{31}P and ^{11}B MAS NMR spectroscopy. TiO_2 incorporates into the glass structure, which results in a decrease in the molar volume and an increase in the glass transition temperature. According to Raman spectra Ti atoms form distorted TiO_6 octahedra and their incorporation into the structural network results in the depolymerization of phosphate chains. ^{11}B NMR spectra of the glasses with increasing TiO_2 content show gradual changes from one symmetrical signal of $B(OP)_4$ units to a broad complex signal which was separated into five signals ascribed to four different types of BO_4 units and one BO_3 unit. With increasing TiO_2 content a part of boron atoms changes from tetrahedral BO_4 to trigonal BO_3 units, which is ascribed to the formation of TiO_6 units in the glass structure.
© 2005 Elsevier Inc. All rights reserved.

Keywords: Borophosphate glasses; Raman spectra; NMR spectra; Titanium dioxide; Glass structure

1. Introduction

Phosphate, borate and borophosphate glasses doped with TiO_2 have been studied in recent years for their possible technological applications associated mainly with their non-linear optical properties [1]. Therefore, there is also a great interest in the study of the structure and properties of various glass-forming systems based on P_2O_5 and TiO_2. Spectroscopic studies of phosphate-based glasses doped with titanium dioxide TiO_2 were reported in [2–5]. In these glasses, TiO_2 behaves as intermediate network former and contributes to the stabilization of the phosphate network and thus relatively large glass-forming regions were reported [2,3]. The incorporation of TiO_x polyhedra into the structural network was realized mostly with the formation of TiO_6 octahedra [1,2,4] or TiO_5 distorted polyhedra [3]. The previous study of $PbO–B_2O_3–P_2O_5–TiO_2$ glasses [4] showed that the incorporation of TiO_2 into the borophosphate glasses is improved by small additions of B_2O_3 (about 10 mol% B_2O_3) in comparison with lead phosphate glasses. Therefore, for the study of the effect of TiO_2 on zinc borophosphate glasses we have chosen $50ZnO–10B_2O_3–40P_2O_5$ as a starting glass composition. This contribution deals with the preparation and study of the effect of TiO_2 on the structure and properties of the Zn borophosphate glass.

2. Experimental

Glasses of the $50ZnO–10B_2O_3–40P_2O_5 + xTiO_2$ system were prepared from ZnO, H_3BO_3, H_3PO_4 and TiO_2 by heating the reaction mixture up to 1200–1300 °C in a Pt crucible, followed by cooling the melt in air or by quenching between two copper blocks to the room

*Corresponding author. Fax: +420 466037068.
E-mail address:* ladislav.koudelka@upce.cz (L. Koudelka).

temperature. The glasses were separately annealed for 60 min at a temperature of 10 K above their T_g and then slowly cooled to room temperature to improve their mechanical properties. The glass density, ρ, was determined on bulk samples by the Archimedes method using CCl_4 as the immersion liquid. The molar volume, V_M, was calculated using the expression $V_M = \bar{M}/\rho$. From the thermomechanical analysis the values of the thermal expansion coefficient, α, the glass transition temperature, T_g, and the dilatation softening temperature, T_d, were determined.

Raman spectra were measured on an FT IR spectrometer, Bruker model IFS 55, with the Raman attachment, FRA 106, under excitation with a Nd:YAG laser radiation using a slit width of $4\,cm^{-1}$ with the power of 300 mW at the sample surface. The Raman spectra were measured at room temperature on bulk samples using 400 scans.

^{31}P and ^{11}B MAS NMR spectra were measured on a BRUKER Avance 400 spectrometer equipped with a standard 1H-X probe with 4 mm rotors. The Larmor frequencies were 161.9 and 128.4 MHz for ^{31}P and ^{11}B, respectively. Pulse length of $1\,\mu s$ was used for ^{31}P, corresponding to $\pi/9$. To avoid background signals from the boron nitride stator, a rotorsynchronized echo was used for the detection with selective pulse lengths of 20 and $40\,\mu s$ for the first and the second pulse, respectively. In total, 32–128 scans were typically used to obtain a correct signal to noise ratio. The recycle delay was 10 s for ^{11}B MAS NMR and 20 s for the ^{31}P MAS NMR measurements, which were sufficient to enable relaxation. ^{31}P chemical shifts are referenced to an 85% H_3PO_4 solution, those of ^{11}B to BPO_4 used as a secondary reference at—30 ppm. In the present manuscript, negative shifts are upfield (shielded), according to the delta convention reported by Levitt [6].

The Q^n notation introduced by Van Wazer [7] is used in this paper: n is the number of bridging oxygen atoms bonded to a given PO_4 sites, i.e., Q^2 is the metaphosphate unit with two bridging oxygen atoms and Q^1 is the end unit with one bridging oxygen atom.

3. Results

By slow cooling of the melt in air we have obtained homogeneous $50ZnO–10B_2O_3–40P_2O_5 + xTiO_2$ glasses in the concentration region of $x = 0–24\,mol\%$ TiO_2 and by quenching between copper plates in the region of $x = 28–64\,mol\%$ TiO_2. The color of the doped glasses slowly changed from clear to yellowish and brown with increasing TiO_2 content. The density of the doped borophosphate glasses increases slightly with increasing content of TiO_2, whereas the molar volume of the glasses steadily decreases (see Table 1). The values of glass transition temperature T_g increase significantly

Table 1
Molar fraction of TiO_2, density (ρ), molar volume (V_M), glass transition temperature (T_g), dilatation softening temperature (T_d) of $50ZnO–10B_2O_3–40P_2O_5 + xTiO_2$ glasses

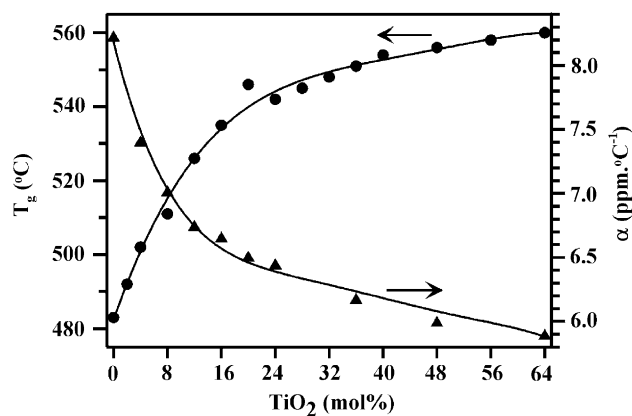| x (mol%)	ρ (g cm^{-3})	V_M (cm^3)	T_g (°C)	T_d (°C)
0	3.14	33.26	483	517
2	3.16	32.85	492	550
4	3.18	32.52	502	561
8	3.21	31.93	511	571
12	3.25	31.35	526	583
16	3.26	30.93	535	579
24	3.30	30.23	542	597
28	3.31	29.95	545	600
32	3.31	29.71	548	607
36	3.32	29.67	551	602
40	3.32	29.58	554	600
48	3.33	29.29	556	614
56	3.34	28.65	558	613
64	3.35	28.28	560	617

Fig. 1. Compositional dependences of the glass transition temperature T_g and the thermal expansion coefficient α in the glass series $50ZnO–10B_2O_3–40P_2O_5 + xTiO_2$.

with increasing TiO_2 content (see Fig. 1). The observed increase in T_g is more steep for the slowly cooled samples, having the composition of $x = 0–24\,mol\%$ TiO_2 (T_g increases from 483 to 557 °C). For the samples prepared by quenching ($x = 28–64\,mol\%$ TiO_2) the increase in T_g is smaller (from 542 to 560 °C). Similar trends were revealed for the data on the dilatometric softening temperature T_d (Table 1).

On the other side, thermal expansion coefficient, α, with increasing content of titania decreases at first sharply within the concentration range 0–12 mol% TiO_2, while at higher titania concentrations the decrease of α slower (see Fig. 1).

Raman spectra of the $50ZnO–10B_2O_3–40P_2O_5 + x$ TiO_2 glasses are shown in Fig. 2 for the concentration region of $x = 0–24\,mol\%$ TiO_2 and in Fig. 3 for the region of 28–64 mol% TiO_2. The spectrum of the $50ZnO–10B_2O_3–40P_2O_5$ borophosphate glass shows
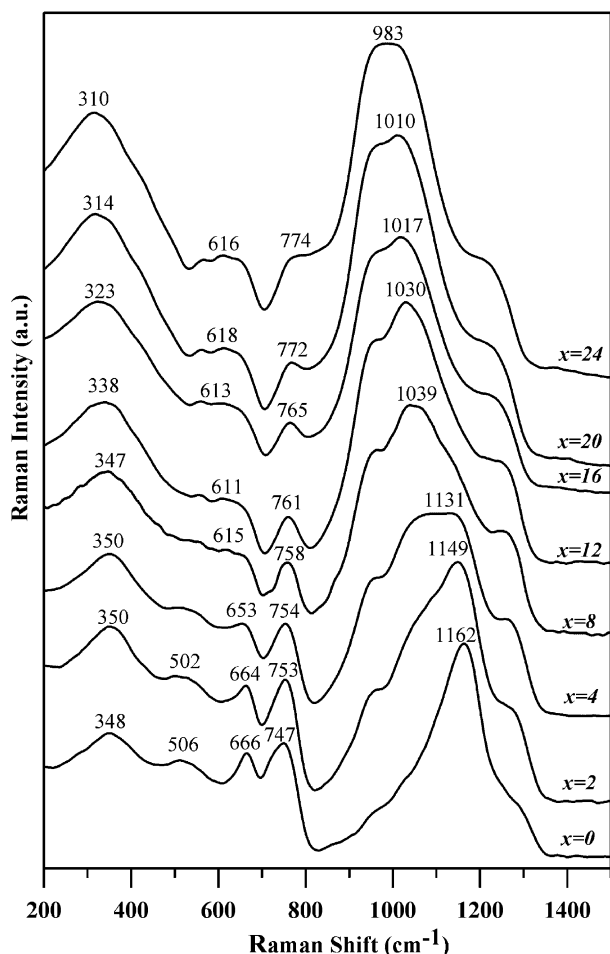
Fig. 2. Raman spectra $50ZnO–10B_2O_3–40P_2O_5 + xTiO_2$ glasses for the samples with $x = 0–24$ mol% TiO_2.

Fig. 3. Raman spectra $50ZnO–10B_2O_3–40P_2O_5 + xTiO_2$ glasses for the samples with $x = 28–64$ mol% TiO_2.

one broad band in the high-frequency region with a maximum at $1162 \, cm^{-1}$ and two medium bands in the middle-frequency region peaking at 747 and $666 \, cm^{-1}$. In the region with a low TiO_2 content of $x = 0–12$ mol% TiO_2 (Fig. 2) the shape and the position structure of the dominant high-frequency Raman band observed in the region of $900–1400 \, cm^{-1}$ changes very significantly, whereas in the glasses with a higher TiO_2 content the high-frequency band shifts slowly to lower wavenumbers up to $979 \, cm^{-1}$ at the glass with $x = 64$ mol% TiO_2. In TiO_2-rich glasses (Fig. 3) with increasing x another two strong bands at 798 and $652 \, cm^{-1}$ and a strong band in the region of deformation vibrations at $304 \, cm^{-1}$ grow significantly with increasing x.

^{31}P MAS NMR spectra (Fig. 4) show two overlapping signals at -25 and -16 ppm for the base glass and their shape evolves with increasing TiO_2 into one signal peaking at -16 ppm. The ^{31}P spectra contain a large set of spinning sidebands due to uncomplete elimination of the chemical shift anisotropy at the MAS spinning frequency used. For the sake of clarity, only the
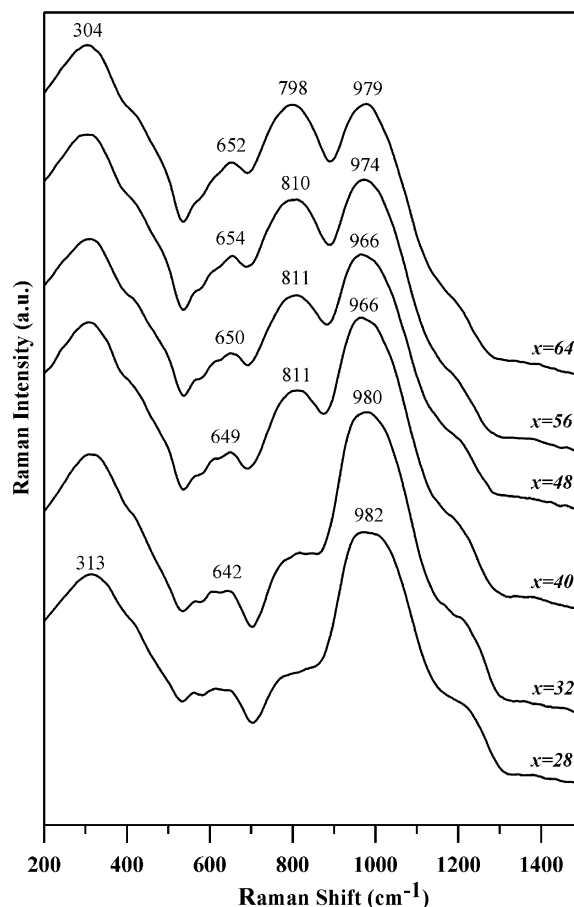
isotropic region is shown on the spectra. The high- and low-frequency wings that appear on some spectra are due to spinning sidebands.

The ^{11}B NMR spectra (Fig. 5) show several BO_4 resonances between -4.2 and 0 ppm, the intensity of the low-field resonances increases progressively at the expense of the high-field ones. In the low-field region a broad signal characteristic of BO_3 site can be seen, which intensity increases with the TiO_2 content.

4. Discussion

A relatively high solubility of TiO_2 in the zinc borophosphate glasses is one of several evidences of its glass-forming behavior in the studied $50ZnO–10$ $B_2O_3–40P_2O_5 + xTiO_2$ glasses. The glass-formation region is larger here than in the similar lead borophosphate glass, where bulk glasses were formed by slow cooling only up to $x = 16$ mol% TiO_2 [4]. Also the observed decrease in the molar volume and increase of the glass transition temperature with increasing TiO_2 content (Table 1) confirm the conclusion that titanium
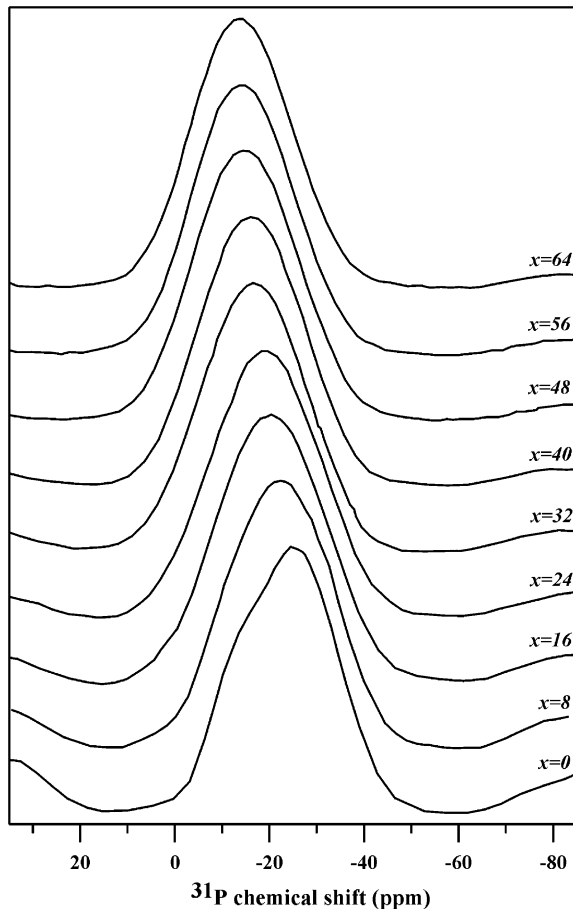
Fig. 4. ^{31}P MAS NMR spectra of the $50ZnO–10B_2O_3–40P_2O_5 + xTiO_2$ glasses for the samples with $x = 0$–64 mol% TiO_2.
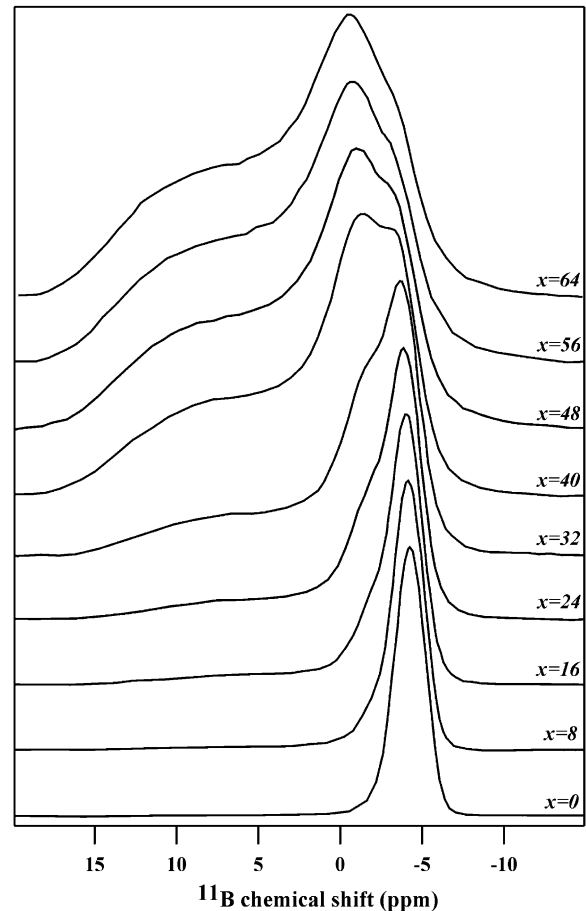
Fig. 5. ^{11}B MAS NMR spectra of the $50ZnO–10B_2O_3–40P_2O_5 + x$-$TiO_2$ glasses for the samples with $x = 0$–64 mol% TiO_2.

dioxide enters the structural network and increases cohesion forces inside the network of the starting $50ZnO–10B_2O_3–40P_2O_5$ glass. The observed trends in oppositional changes in the compositional dependences of the glass transition temperature and the thermal expansion coefficient are similar to those observed recently by Jun et al. [8] in phosphate-based glasses, where the product of T_g and α was found to be a constant.

The yellowish up to brown color of the glasses we ascribe to the presence of small amounts of Ti^{3+} ions in the glasses. Similar coloration of glasses due to the presence of Ti^{3+} ions was observed also in the studies of calcium phosphate glasses with additions of TiO_2 [2]. According to Hashimoto et al. [9] decoloration of the glasses can be done by annealing at temperatures around T_g, which results in the removing of Ti^{3+} ions from the glass.

The coordination of Ti^{4+} ions by oxygen atoms in the studied zinc titanophosphate glasses is reflected in the character of their Raman spectra. The spectra of the TiO_2-rich glasses (Fig. 3) reveal two bands at 798 and 652 cm^{-1}, which can be ascribed to the vibrations of

titanate units TiO_x, because their relative intensity against the high-frequency band at 979 cm^{-1} increases with increasing TiO_2 content. In order to solve the assignment of these two bands we have prepared sodium glass of the composition $50Na_2O–10B_2O_3–40P_2O_5 + 48$ TiO_2 and compared its Raman spectra with the corresponding $50ZnO–10B_2O_3–40P_2O_5 + 48TiO_2$ glass (Fig. 6). Both spectra reveal a similar structure; only the corresponding Raman bands at sodium glass are shifted to lower wavelengths in comparison with the spectra of the zinc glass. Krimi et al. [10] in their study of $Na_2O–TiO_2–P_2O_5$ glasses observed similar bands at 742 and 637 cm^{-1} and ascribed these bands to the vibrations of distorted TiO_6 octahedra. Its shift to higher wavelengths in Zn glasses can be explained by the differences in the ionic field strength of Na^+ and Zn^{2+} cations. Therefore, we suppose that titanium ions form TiO_6 octahedra in the structure of the studied glasses and that the bands of 652 and 798 cm^{-1} in the Raman spectra of Ti-rich glasses Zn borophosphate glasses can be assigned to the vibrations of TiO_6 units. Moreover, the measurement of Raman spectra with the polarized light showed that the band of 798 cm^{-1} is polarized, i.e.,
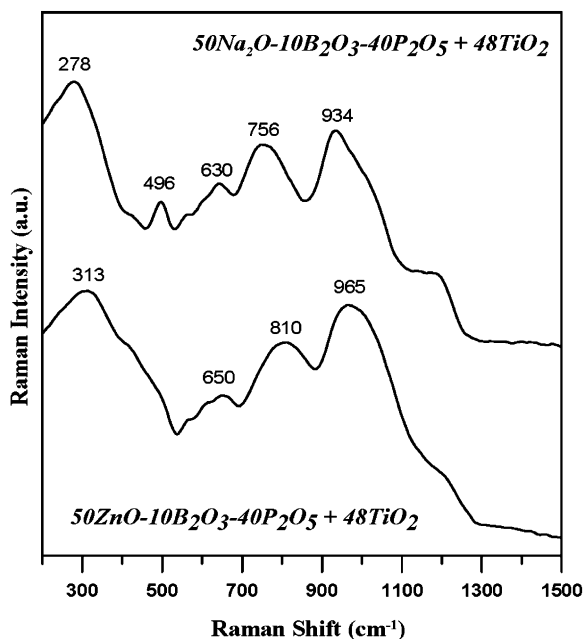
Fig. 6. Comparison of the Raman spectra of 50ZnO–10B$_2$O$_3$–40-P$_2$O$_5$ + 48TiO$_2$ glass and 50Na$_2$O–10B$_2$O$_3$–40P$_2$O$_5$ + 48TiO$_2$ glass.

it corresponds to the totally symmetric vibration of TiO$_6$ units. The smaller band of $496 \, \text{cm}^{-1}$ present in the Raman spectrum of sodium glass is probably overlapped in the Raman spectrum of Zn glass by a broadband of deformation vibrations and can be seen only as a shoulder. This band can be seen also in the Raman spectra of sodium titanophosphate glasses [10], where its assignment was not given. Sakka et al. [11] report the band of $611 \, \text{cm}^{-1}$ as a characteristic for the octahedral coordination of Ti in rutile crystals.

The information on the vibrations of phosphate units can be obtained from the high-frequency part of the Raman spectra. Its evolution in the glasses with a low-TiO$_2$ content (Fig. 2) shows on the depolymerization of phosphate chains, because in the region 0–12 mol% TiO$_2$ its maximum shifts from the region of the vibration of Q^2 units into the region characteristic for the vibrations of Q^1 units [12].

In the parent undoped glass of the composition, 50ZnO–10B$_2$O$_3$–40P$_2$O$_5$ this band is accompanied by two medium bands peaking at 666 and $747 \, \text{cm}^{-1}$ ascribed to the vibrations of bridging oxygen atoms in the Q^2 chains and Q^1 units, respectively [12]. The band of $666 \, \text{cm}^{-1}$, characteristic for the vibrations of bridging oxygen atoms between metaphosphate units [13], vanishes within the concentration region of $x = 0$–8 mol% TiO$_2$ simultaneously with increasing content of Q^1 units. On the other side the band of $747 \, \text{cm}^{-1}$ shifts to higher wavenumbers up to $772 \, \text{cm}^{-1}$ at the glass with $x = 20$ mol% TiO$_2$ showing on the presence of Q^1 units.

This evolution of the Raman spectra we ascribe to the interruption of metaphosphate chains by the insertion of TiO$_6$ units. The dominant band of the stretching vibrations of phosphate units changes its character also at the glasses with a higher TiO$_2$ content, where the strength of the band at 1030–1040 cm^{-1} decreases and the strength of the band 966–980 cm^{-1} increases. The latter band approaches the region characteristic of the vibrations of Q^0 (orthophosphate) units in the solid orthophosphates [14]. Therefore, we cannot exclude that in the TiO$_2$-rich glasses some phosphate groups are isolated by titanate or borate groups.

^{31}P MAS NMR spectra (Fig. 4) of the parent glass of the composition 50ZnO–10B$_2$O$_3$–40P$_2$O$_5$ reveals one broad resonancy composed of two signals with maxima at $\delta = -25$ ppm -16 ppm. With increasing content of TiO$_2$ the strength of the second maxima increases, while that of the first maxima decreases and the maximum of the first signal shifts downfield. These changes in the NMR spectra are associated with the depolymerization of the borophosphate network and the formation of Q^1 sites bonded to TiO$_6$ polyhedra. We note that in these borophosphate glasses, Q^1 and Q^2 sites may be linked to either another phosphate unit, or to a borate unit (BO$_4$ or BO$_3$). The broad distribution of chemical shifts does not enable to distinguish a possible small amount of the Q^0 units the presence of which cannot be excluded according to the Raman spectra. This ^{31}P chemical shift distribution originates from the distribution of bond lengthes and angles, which are inherent to the amorphous state.

^{11}B MAS NMR spectra (Fig. 5) of the parent glass of the composition 50ZnO–10B$_2$O$_3$–40P$_2$O$_5$ show one symmetrical signal at -4.3 ppm, characteristic of BO$_4$ units coordinated by four phosphorus atoms [15]. With increasing TiO$_2$ content the structure of the NMR signal changes very significantly. In the region of positive values of the chemical shift the resonancy characteristic of BO$_3$ units [16] appears in the NMR spectra showing on the change in the coordination of boron atoms from tetrahedral BO$_4$ to three-coordinated in BO$_3$ units. The starting symmetric resonancy of BO$_4$ units also changes its structure, which can be separated into four signals reflecting four different coordinations of boron atoms. Thus we have decomposed the obtained ^{11}B MAS NMR spectra into individual components corresponding to the structural units identified with these spectra—B(OP)$_4$ at -4.27 ppm, B(OP)$_3$(O–Zn,Ti) at -2.5 ppm, B(OP)$_2$(O–Zn, Ti)$_2$, at -0.3 ppm, B(OP)$_1$O(Zn, Ti)$_3$ at 2.3 ppm and BO$_3$ units at 10.6 ppm. An example of the fit is shown in Fig. 7 for the glass composition 50ZnO–10B$_2$O$_3$–40P$_2$O$_5$ + 48 TiO$_2$. The BO$_3$ resonance is fitted with a second-order quadrupolar lineshape with typical characteristics (Cq = 2.4 MHz, $\eta q = 0.5$). BO$_4$ are fitted with Gaussian lineshape, meaning that they are submitted to a very
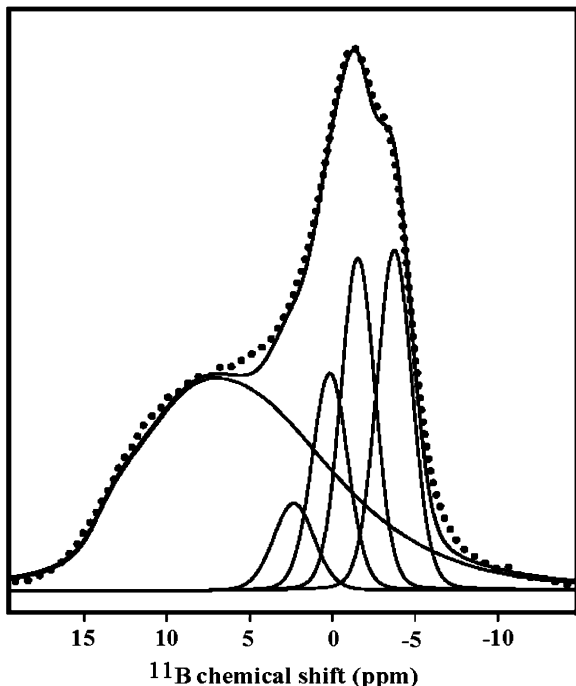
Fig. 7. Example of the decomposition of ^{11}B MAS NMR spectra of the $50ZnO–10B_2O_3–40P_2O_5 + 48TiO_2$ glass. Dotted line: experimental spectrum, continuous lines: individual components and fitted spectrum.

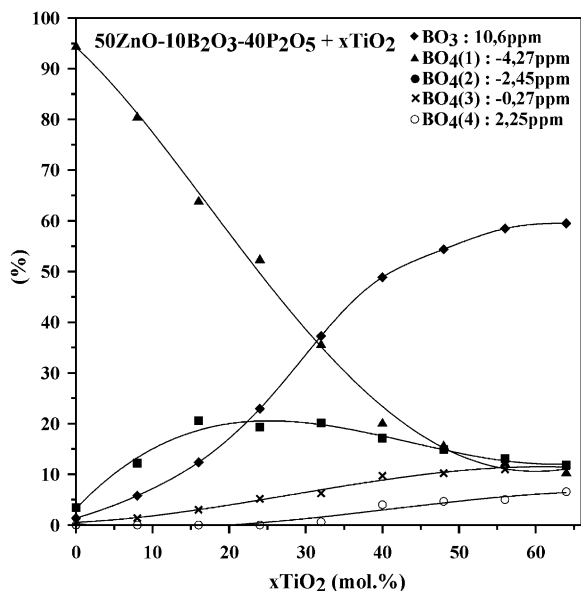Fig. 8. The compositional dependence of the relative amount of basic structural borate units in $50ZnO–10B_2O_3–40P_2O_5 + xTiO_2$ glasses for the samples with $x = 0–64$ mol% TiO_2 as obtained by the fit of ^{11}B MAS NMR spectra.

small quadrupolar effect. The existence of the 4th site—assigned to $B(OP)_1O(Zn, Ti)_3$ at 2.3 ppm is, however, not sure since its presence is only indicated by an optimization of the fit, not by a singularity on the spectra. The attributions are justified by considering that the incorporation of TiO_2 into the borophosphate network creates new non-bridging oxygen atoms, which are at the origin of the different BO_4 sites. From the compositional dependence of the number of individual borate units (see Fig. 8) we can see that with increasing TiO_2 content the number of BO_3 units steadily increases, whereas the number of BO_4 units decreases. This effect can be described by the equation

$$BO_{4/2} + TiO_{4/2} = BO_{3/2} + TiO_{6/2}. \tag{1}$$
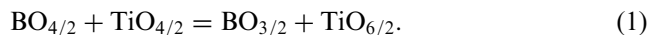
This equation corresponds to the results of Raman spectra, which showed on the presence of TiO_6 octahedra in the structural network. Titanium dioxide brings stoichometrically two oxygen atoms in $TiO_{4/2}$ and needs an additional oxygen atom for the formation of $TiO_{6/2}$ octahedra. This additional oxygen atom is evidently taken off from the boron coordination and thus boron atoms transfer one oxygen atom to titanium and convert their $BO_{4/2}$ coordination into $BO_{3/2}$ coordination.

5. Conclusion

The doping of zinc borophosphate glasses with TiO_2 showed that the titanium dioxide plays here the role of an intermediate oxide, which incorporates into the structural network. This incorporation increases bonding forces inside the network, which is reflected in increasing values of glass transformation temperature. A relatively high content of TiO_2 in these glasses resulted in the appearance of distinct vibrational bands of titanate structural units in the Raman spectra. The formation of TiO_6 octahedra inside the network resulted in the depolymerization of phosphate and borate chains. Such a high coordination number of Ti demanded a high number of bonding oxygen atoms which could explain the observed changes in the coordination of boron in these glasses, where according to the ^{11}B MAS NMR spectra with increasing incorporation of TiO_2 into the glass structure the tetrahedral BO_4 units are gradually replaced by trigonal BO_3 units.

Acknowledgments

References

[1] E. Fargin, Phosphorus Res. Bull. 10 (1999) 490–496.

[2] R.L. Brow, D.R. Tallant, W.L. Warren, A. McIntyre, D.E. Day, Phys. Chem. Glasses 38 (1997) 300–306.

[3] L. Montagne, G. Palavit, A. Shaim, M. Et-Tabirou, P. Hartmann, C. Jäger, J. Non-Cryst. Solids 293–295 (2001) 719–725.

[4] L. Koudelka, P. Mošner, M. Zeyer, C. Jäger, J. Non-Cryst. Solids 326–327 (2003) 72–76.

[5] L. Montagne, S. Daviero, G. Palavit, A. Shaim, M. Et-Tabirou, Chem. Mater. 115 (2003) 4709–4716.

[6] M. Levitt, J. Magn. Reson. 126 (1997) 164–182.

[7] V. Wazer, Phosphorus and its Compounds, vols. 1 and 2, Interscience, New York, 1951.

[8] J.S. Jun, M.R. Cha, B.H. Jung, H.S. Kim, J. Korean Ceram. Soc. 40 (2003) 1127–1131.

[9] T. Hashimoto, H. Nasu, Y. Kamiza, Abstracts XX International Congress on Glass, Kyoto, The Ceramic Society of Japan, Kyoto, 2004, p. 133.

[10] S. Krimi, A. El Jazouli, L. Rabardel, M. Couzi, L. Mansouri, G. Le Flem, J. Solid State Chem. 102 (1993) 400–407.

[11] S. Sakka, F. Mizaji, K. Fukumi, J. Non-Cryst. Solids 112 (1989) 64–68.

[12] V. Fawcett, D.A. Long, L.H. Taylor, Proceedings of the 5th International Conference of Raman Spectroscopy, Freiburg, Hans Ferdinand Schulz Verlag, Freiburg/Br. 1976, pp. 112–113.

[13] Ya.S. Bobovich, Opt. Spektrosk. 13 (1962) 492–497.

[14] R.A. Nyquist, C.L. Putzig, M.A. Leugers, The Handbook of Infrared and Raman Spectra of Inorganic Compounds and Organic Salts, vol. 1, Academic Press, New York, 1997.

[15] R.K. Brow, D.R. Tallant, J. Non-Cryst. Solids 222 (1997) 396–406.

[16] J.F. Ducel, J.J. Videau, K.S. Suh, J. Senegas, Phys. Chem. Glasses 35 (1994) 10–16.